

Effects of Cross-Linking on Proton Spin-Lattice Relaxation in Polybutadiene

T. J. Rowland* and L. C. Labun

Materials Research Laboratory and Department of Metallurgy and Mining Engineering, University of Illinois at Urbana-Champaign, Urbana, Illinois 61801.
Received September 6, 1977

ABSTRACT: A marked decrease in proton spin-lattice relaxation time T_1 at temperatures above the T_1 minimum is observed in cross-linked polybutadiene and is interpreted in terms of a broad distribution of relaxation times attributed to the protons in regions near the chemical cross-link. This distribution results from segmental motional correlation times ranging upward from the correlation time of a free chain at that temperature to times at least one to two orders of magnitude longer.

I. Introduction

This paper reports the results of experiments in which the proton spin-lattice relaxation time T_1 in cross-linked *cis*-1,4-polybutadiene (PB) is studied as a function of cross-link density and temperature. Our objective is to relate PB network chain dynamics to network structure and chain length. The early NMR studies of Gutowsky et al.^{1,2} on sulfur vulcanized natural rubber revealed many of the salient features of proton resonance in these systems, pointing out the difficulties of interpretation and the apparent inconsistencies which appear when the results of the BPP theory³ of nuclear relaxation are applied to them.

The experimental aspects of this investigation are summarized in section II; in section III the results are presented in the form of T_1 vs. inverse temperature and T_1 vs. cross-link density at fixed temperature. The model which we adopt together with the interpretation of the data is included in section III.

II. Experimental Section

Apparatus. All of the spin-lattice relaxation times were measured using a pulsed spectrometer of standard design working at the fixed frequency of 9.0 MHz. A single-coil proton-free probe was constructed and used in a transmit-receive configuration over the temperature region from -100 to $+95$ °C. A $180-\tau-90$ sequence was used in the null technique for measuring T_1 after first determining that the decay was exponential. Data were accumulated in a signal averager in all instances and the amplitude of the signal was plotted against τ over a small region around the null in magnetization; T_1 is equal to $\tau_{\text{null}}/\ln 2$.

Specimen Preparation and Characterization. All specimens were produced from Ameripol CB-220 stated to be >98% *cis*-1,4-polybutadiene. The CB-220 was dissolved in benzene, reprecipitated by methanol, and dried to remove antioxidant prior to cross-linking procedure. The initiator was dicumyl peroxide (DCP) which had been dissolved in a small amount of benzene and added to a benzene solution of CB-220. These were stirred together 12 h or more following which the benzene was evaporated to give a uniform distribution of DCP in polymer. The mixture thus prepared was heated in the mold of a metallographic sample press first to 90 °C for 30 min and finally to 140 °C for 45 min, under a pressure of about 4000 lb/in.²; the samples were then cooled. They weighed 1.5 to 2 g and were in the form of thin disks 2–3 mm thick and 2.54 or 3.18 cm in diameter.

Following the cross-linking process each disk was extracted with benzene (frequently changed) for 48 h. Its diameter in the swollen state D_s was measured at the end of this treatment. The disk was then deswollen with methanol and dried under vacuum, and its diameter dry D_d was measured. The network chain density ν_e of the sample is given in terms of ν_2 , the volume fraction polymer in the swollen network in equilibrium with excess solvent, χ , the polymer-solvent interaction parameter, and V_1 , the molar volume of the solvent,⁵

$$\nu_e = \frac{\ln(1 - \nu_2) + \nu_2 + \chi \nu_2^2}{V_1(A\nu_2^{1/3} - B\nu_2)} \quad (1)$$

with $A = 1$, $B = 0.5$, and $\nu_2 = (D_d/D_s)^3$.

The solvent-polymer interaction parameter χ for benzene-PB was determined by using χ_D for decane-PB determined by Loan⁶ to find ν_e for a cross-linked sample which was then used as a "transfer standard" from which to evaluate χ . Repetition of this procedure on a second independent specimen reproduced the result within 2.8%. We adopt the value found, $\chi = 0.387 \pm 0.020$, for use in all subsequent calculations involving eq 1.⁷

In Table I we list the samples together with their characterization in terms of DCP concentration (in mol of DCP per cm³ of PB in the mixture prior to cross-linking), the measured swelling ratio D_d/D_s , the network chain density ν_e according to eq 1, the apparent cross-linking efficiency $E_{\text{xl}} = \nu_e/(\text{conc DCP})$, and the average number of repeat units (RU) per network chain N_m corresponding to ν_e ; $N_m = 0.0187/\nu_e$, where 0.0187 is the mol of RU of PB per cm³. Our considerations of the behavior of E_{xl} at low N_m , and the steric requirements of a tightly cross-linked network, led us to estimate adjusted values of N_m for the most highly cross-linked samples; these are listed as the numbers N . For chain lengths less than about seven RU these corrections are substantial and N should be regarded as a reasoned estimate only. It may be noted that $\rho_x = \nu_e/2$ where ρ_x is the cross-link density in mol of cross-link per cm³ for a network of tetrafunctional cross-links.

Following the final vacuum drying procedure sections of the samples were sealed under dry nitrogen into glass vials for the measurement of T_1 .

III. Results and Interpretation

Curves representing the experimentally measured spin-lattice relaxation times for a selected group of the samples listed in Table I are plotted against inverse temperature in Figure 1. With increasing cross-link density the $\log T_1$ vs. $1/T$ curves are seen to change markedly as follows: (i) At a sufficiently high fixed temperature, the effect of increasing the cross-link density ρ_x is to monotonically decrease the relaxation time (rather drastically for high ρ_x). (ii) For network chain lengths greater than about 20 RU the minimum in T_1 is not perceptibly changed in position or magnitude by changes in cross-link density. (iii) T_1 in the low-temperature region ($T < T_{\text{min}}$) is much less strongly influenced by cross-linking, and in particular the slopes of the lines describing $\log T_1$ vs. $1/T$ in that region are approximately independent of network chain length down to lengths of approximately 10 RU. For $N \lesssim 10$ RU in this temperature range the values of T_1 increase as chain length decreases. Also for $N \lesssim 10$ RU the value of $T_{1 \text{ min}}$ is seen to increase and move to the left, toward higher temperatures in Figure 1.

In Figure 2 the data are displayed in the form $\log T_1$ vs. the logarithm of average network chain length N at several fixed temperatures above -39 °C, T_{min} for CB-220. The gradual upturn at the left is associated with the increase in the minimum value of T_1 as well as the shift in T_{min} of highly cross-linked samples. The dominant behavior in the temperature region $0 \lesssim T \lesssim 95$ °C is a monotonic decrease in T_1 as the average network chain length N grows smaller.

Our explanation of this behavior is as follows. In the high-

Table I
List of Samples Together with Their Characterization in Terms of Initiator Concentration, Linear Swelling Ratio, and Network Chain Concentration after Cross-Linking ν_e^a

Sample	Concn of DCP, 10^{-4} mol/cm ³	D_d/D_s	ν_e , 10^{-4} mol/cm ³	E_{xl}	N_m	N
18	0.0485	0.489	0.555	11.4	337	337
17	0.131	0.555	1.25	9.5	149	149
16	0.336	0.625	2.84	8.5	66	66
15	0.498	0.660	4.23	8.5	44	44
12	0.505	0.664	4.45	8.8	42	42
14	0.679	0.674	4.99	7.3	37	37
11	0.978	0.760	13.4	13.7	14	14
9	2.04	0.813	25.3	12.4	7.4	7.9
19	2.28	0.820	26.7	11.7	7.0	7.5
3	2.45	0.846	38.1	15.6	4.9	5.7
8	4.01	0.904	82.2	20.5	2.3	3.8
6	8.72	0.98	326.	37.4	0.6	2.8

^a N is the average number of repeat units per network chain (see text).

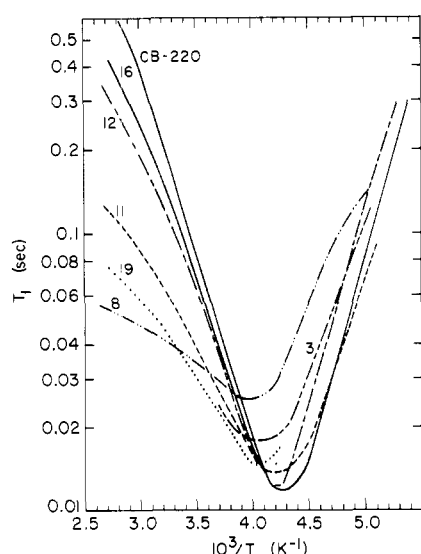


Figure 1. Summary presentation of the temperature dependence of T_1 for uncross-linked PB (CB-220) and several cross-linked samples described by number in Table I. Measurements were made at 9.0 MHz.

temperature region, at 90 °C for example, moderately low cross-link densities of 0.2×10^{-4} mol/cm³ decrease the relaxation times measurably; a 50% reduction occurs for $N = 50$ RU ($\rho_x = 2 \times 10^{-4}$ mol/cm³). The introduction of each cross-link decreases the relaxation time by providing an additional contribution to the relaxation. If this decrease were the result of a change in a single correlation time τ_1 , uniform over the sample, it would suggest an increase in τ_1 with cross-link density. The fact that the temperature of the T_1 minimum does not change with cross-link density, and that the low-temperature behavior is largely unaffected, indicates that the additional cross-links are not associated with the increase of a single τ uniform over the system but rather with special sites of rapid high-temperature relaxation. Since we did not observe two or more relaxation times T_1 in the present samples, very good contact must exist between the proposed relaxation sites and the chains joining them. Our model is thus one in which a cross-link introduces a relaxation site. Physically the proton sites having the shortest T_1 may lie near, but not necessarily at, the chemical cross-link. The most effective site can be associated with protons in chain segments having correlation times approximating ω_0^{-1} ; its location depends upon the chain dynamics in the vicinity of the chemical cross-link and in particular the contour distance from the cross-link. We define

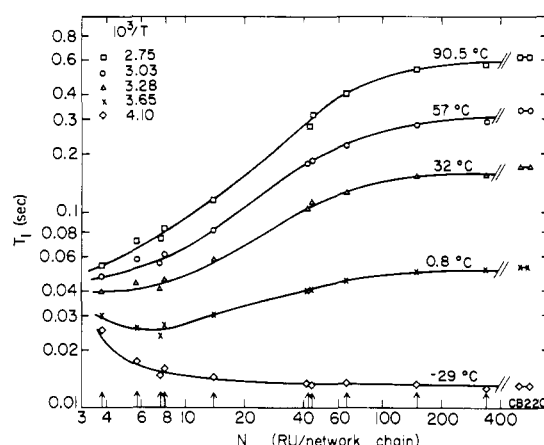


Figure 2. Plot of relaxation time as a function of average network chain length N at several fixed temperatures above -39 °C (the temperature of the T_1 minimum for CB-220). T_1 decreases monotonically with decreasing N for most values of N and T portrayed. The arrows on the abscissa indicate samples listed in Table I.

a "cross-link region", within which the segmental motion is strongly perturbed, and treat it separately from those sections of network chains between such regions and lying completely outside of them. The latter are treated as free chains with lattice relaxation properties identical with those of pure PB. Spin diffusion along chains within the cross-link region implies the existence of a local T_{1k} which may vary with position along the chain. We distinguish between the direct T_1 process in which energy is lost from link k directly to the lattice and the indirect T_1 process by which the z component of magnetization at link k is decreased by spin diffusion to the sink. T_{1k} is the result of both of these processes acting in parallel at each proton along the chain. In the network non-equivalent proton sites having different T_{1k} are not resolved because of the short spin-spin relaxation times. We propose to differentiate between only the chain protons and the cross-link protons and to characterize a distribution of T_{1k} within the cross-link region resulting from a distribution of segmental correlation times within that region.

It is known that polymers in general,⁸ and specifically polybutadiene^{9,10} in the temperature region above its glass transition temperature T_g , exhibit spin-spin relaxation times which are very much less than the values of T_1 at the same temperature. Throughout the temperature region of interest to us $T_2 \ll T_1$ for all samples although we are well into the "line narrowing" regime; T_2 has a maximum value of about 1 ms for uncross-linked CB-220 and it is shorter for all cross-

linked samples. There is good contact of each network proton with its neighbors, and energy is transferred predominantly along chains to the cross-link regions. Under these circumstances the observed relaxation rate

$$T_1^{-1} = \sum_k P_k T_1^{-1}(\tau_k) \quad (2)$$

where P_k is the fraction of nuclei in sites with relaxation times $T_{1k} = T_1(\tau_k)$ and $\sum_k P_k = 1$. T_{1k}^{-1} is, as previously defined, the total spin-lattice relaxation rate for a nucleus in the k th site. In practice, for temperatures higher than T_{\min} the most effective τ_k in causing relaxation are always longer than the uncross-linked chain correlation time τ_c ; these longer τ_k appear to be introduced by the cross-link. All nuclei near the chemical cross-link have very short T_2 (probably 10–100 μsec^{10}), and since they lie *within* a small region containing repeat units whose τ_k are greater than τ_c and may include ω_0^{-1} , they can be said to relax as a unit with the single relaxation rate $T_{1x}^{-1} = \sum_k x P_k T_{1k}^{-1}$. The superscript x on the summation indicates that this sum is over only those sites inside of the cross-link region. Thus, to a first approximation, eq 2 becomes

$$T_1^{-1} = v_x T_{1x}^{-1} + v_c T_{1c}^{-1} \quad (3)$$

where v_x is the mole fraction of repeat units in the cross-links and $v_c = (1 - v_x)$ is the fraction in chains, i.e., not in cross-links. T_{1c} is the spin-lattice relaxation time for protons in the chains. Equation 3 is valid for $v_x \lesssim 0.3$. Its form is a result of the rapid mixing caused by $T_2 \ll T_1$.

A rough estimate of T_{1x} can be obtained at any temperature by noting the relaxation time for a highly cross-linked sample; at 90.5 °C for example it can be inferred that $T_{1x} < 54$ ms, the value obtained for our sample 8. In this temperature region $T_2 \ll T_{1x} < T_{1c}$, and this approach adequately explains the data for all moderate cross-link densities ($v_x \lesssim 0.3$). The most closely similar application of this model appears to be Crist's treatment of the branch point protons in branched polyethylene.¹¹

We have obtained the cross-link relaxation time T_{1x} from the observed T_1 vs. cross-link density data at several fixed temperatures using eq 3 in the form $(T_1^{-1} - T_{1c}^{-1}) = v_x(T_{1x}^{-1} - T_{1c}^{-1})$; the results are shown in Figure 3. In deriving T_{1x} from the data we have let each cross-link region consist of six repeat units and assumed tetrafunctional cross-links. Thus v_x is given by $3/N$, and N for each sample is given in Table I. T_1 and T_{1c} are the observed value for the sample and for CB-220 respectively at the same temperature. A second least-squares analysis was run assuming T_{1c} to be unknown and obtaining both T_{1x} and T_{1c} from eq 13 plotted as T_1^{-1} vs. v_x . With the exception of the highest temperature point ($10^3/T = 2.75$) the resulting T_{1c} agreed very closely ($\leq 7\%$) with the measured values which are estimated to be correct within $\pm 5\%$. This good agreement corroborates our assumption that in applying eq 3 T_{1c} of a cross-linked network is well approximated by T_1 of CB-220, i.e., uncross-linked PB. The model appears applicable to all temperatures; it is clear however that somewhere to the right of the T_1 minimum for cross-linked samples the cross-links become regions of slow relaxation relaxing to the generally larger volume of almost homogeneous network chains. The values of T_{1x} increase very rapidly in this region, as Figure 3 shows; still the T_{1c} , determined from the T_1 vs. v_x of cross-linked samples, agree with the measured value for CB-220 within the tolerances given above. The treatment is inherently limited to a "dilute" region of cross-link density in which the cross-links are noninteracting and are separated by lengths of PB chain which are essentially unperturbed. The relaxation per cross-link is found to be independent of cross-link concentration for $v_x \lesssim 0.3$ and very nearly so for $v_x \lesssim 0.4$.

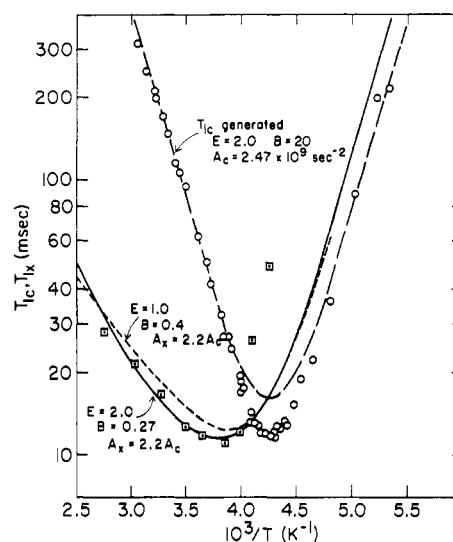


Figure 3. Spin-lattice relaxation of protons at 9 MHz in uncross-linked PB (○), T_{1c} , and in small regions surrounding cross-links T_{1x} in networks (□) as a function of inverse temperature. The long-dashed curve analytically simulates much of the CB-220 data. The full and short-dashed curves are the result of ascribing certain motional correlation time distributions to the protons near a cross-link (see text).

Having decomposed the network T_1 into two components, corresponding to the cross-link regions and the chains, we seek to understand the main features of the cross-link relaxation curve, namely its low slope in the high-temperature region, its position on the temperature axis, the magnitude of the T_{1x} values, and its pronounced asymmetry. Although the curve is very different from the classic $\log T_1$ vs. $1/T$ curve for a liquid of low molecular weight, the BPP theory remains a logical point of departure in understanding its features. The presence of a distinct minimum in the T_{1x} vs. $1/T$ curve shows that an optimum condition exists for relaxation; the asymmetry around T_{\min} is the major feature requiring explanation.

Physical considerations outlined above lead us to expect that within the cross-link region, no correlation time shorter than that of pure uncross-linked PB chains τ_c will exist. The distribution of τ will thus begin at τ_c and extend toward longer τ . We use the modified BPP expression^{1,3,12,13}

$$\frac{1}{T_1} = \frac{3\gamma^4\hbar^2}{10} \sum_j r_j^{-6} \left[\frac{\tau}{1 + \omega_0^2\tau^2} + \frac{4\tau}{1 + 4\omega_0^2\tau^2} \right] = AF(\omega_0, \tau) \quad (4)$$

to relate a motional correlation time τ to the proton relaxation rate T_1^{-1} at angular frequency ω_0 . Here γ is the proton gyromagnetic ratio, \hbar is Planck's constant divided by 2π , and the r_j are internuclear distances to the other protons in the system. ^{13}C contributions to the relaxation are negligible. To establish an analytic form for τ_c we first attempt to simulate the $\log T_{1c}$ vs. $1/T$ curve for CB-220. If we assume τ_c to be of the form $\tau_c = \tau_0 \exp(E_0/RT)$, eq 4 is incapable of a good fit to the data for CB-220 in the immediate region of the T_{1c} minimum,¹ but the straight line sections of the $\log T_{1c}$ vs. $1/T$ data are described reasonably well. The slopes of the high- and low-temperature straight-line segments differ somewhat ($E_0/R = 3073\text{K}$ and 3354K respectively), and the E_0 are believed *not* to represent activation energies in this case.^{14,15} Using $E_0/R = 3214\text{K}$, $\tau_0 = 1.2 \times 10^{-4}$ s [from the condition $\tau_c = 0.6158\omega_0$ at the T_1 minimum], and $A = A_c = 2.47 \times 10^9 \text{ s}^{-2}$ a useable analytical representation of our T_{1c} vs. $1/T$ data for CB-220 is achieved. The result of this fitting process is shown in Figure 3.

It remains to choose a function $P(\tau)$ to represent the dis-

tribution of correlation times in the cross-link region. For molecular phenomena in which the range of times is commonly very wide it has been found preferable to use the logarithm of τ as the independent variable rather than τ itself.^{12,16} We consider the Gaussian distribution of $z = \ln(\tau/\tau^*)$ as a trial function. This so-called log-normal distribution is defined somewhat differently in the present treatment; we let

$$\begin{aligned} P(\tau) d\tau &= H(z) dz = (2B\pi^{-1/2}) \exp(-B^2 z^2) dz \\ &= 0 \quad \tau > \tau^* \quad (z \geq 0) \\ &= 0 \quad \tau < \tau^* \quad (z < 0) \end{aligned}$$

$$\int_0^\infty P(\tau) d\tau = \int_{-\infty}^\infty H(z) dz = 1. \quad (5)$$

The breadth parameter B determines the width of the distribution and is related to the rms deviation of z from $z = 0$ by $z = 1/(2^{1/2}B)$. The average value of τ is just

$$\bar{\tau} = \int_0^\infty \tau P(\tau) d\tau = 2B\tau^* \pi^{-1/2} \int_0^\infty \exp(z - B^2 z^2) dz \quad (6)$$

From eq 2 and 3 the relaxation rate T_{1x}^{-1} resulting from the distribution of correlation times $P(\tau)$ in the cross-link region is given by

$$\begin{aligned} T_{1x}^{-1} &= A_x \int_0^\infty P(\tau) F(\omega_0, \tau) d\tau \\ &= \frac{2A_x B_x \tau^*}{\pi^{1/2}} \int_0^\infty \exp(z - B_x^2 z^2) \\ &\quad \times \left[\frac{1}{1 + \omega_0^2 \tau^{*2} e^{2z}} + \frac{4}{1 + 4\omega_0^2 \tau^{*2} e^{2z}} \right] dz \quad (7a) \end{aligned} \quad (7)$$

A_x is the value of A appropriate to the protons in a cross-link region. Recalling that τ^* marks the short-time end of the distribution, and that it should be approximately equal to the chain correlation time at any given temperature, we set $\tau^* = \tau_c = \tau_0 \exp(E_0/RT)$ where E_0 and τ_0 are given above. T_{1x} is then calculated by evaluating eq 7a as a function of temperature with the temperature dependence implicit in τ^* . The breadth parameter B_x is adjusted to achieve the best agreement between the calculated and measured T_{1x} vs. $1/T$ curves over the temperature range investigated. The full curve in Figure 3 shows the results using $B_x = 0.27$ and $A_x = 5.43 \times 10^9 \text{ s}^{-2} = 2.2A_c$. In the absence of a theoretical treatment of polymer relaxation capable of describing the shape near the T_1 minimum we attach no physical significance to the relative magnitudes of A_c and A_x ; they are not inconsistent with BPP theory. The computed curve agrees reasonably well with the experimental T_{1x} but curves upward too rapidly at high temperatures. Its minimum lies approximately 25 °C higher than the minimum in T_{1c} in agreement with the T_{1x} data. On the low-temperature side of the minimum, T_{1x} from eq 7a roughly parallels T_{1c} as would be expected in view of the form of $P(\tau)$. The observed cross-link relaxation time, on the other hand, increases very rapidly. The error in decomposing experimental T_1 points is relatively large in this region because T_1 lies close to T_{1c} for all samples with $v_x < 0.3$; nevertheless the sharp increase in T_{1x} appears to be real. This strongly suggests that our $P(\tau)$ places too much emphasis on components near τ_c or that as the temperature is lowered the mobility within the cross-link region decreases more rapidly than function 5 with B_x fixed equal to 0.27. Since the function $P(\tau)$ is not unique and is used primarily as an example of the general form needed to test the model, we do not examine the result of letting B be temperature dependent. The present form of $P(\tau)$ gives a distribution whose width is a fixed multiple of $\tau^* = \tau_c$.

The curvature at high temperatures exhibited by the full curve in Figure 3 is related to the form of our distribution

function, eq 5. As an alternative trial function we let $P(\tau) d\tau = W(z) dz$ where $W(z)$ in our case is a truncated Weibull function¹⁷

$$\begin{aligned} W(z) &= \frac{BE}{\Gamma(1/E)} \exp[-(Bz)^E] \quad 0 \leq z < \infty \\ &= 0 \quad -\infty < z < 0 \end{aligned} \quad (8)$$

with $z = \ln(\tau/\tau^*)$ as above. It is normalized $\int_{-\infty}^\infty W(z) dz = 1$, and the parameter E allows the distribution to be varied smoothly between the Gaussian form (eq 5) and a simple exponential. The result for T_{1x} from eq 7 and 8 when $E = 1$ and $B_x = 0.4$ (Figure 3) shows improved agreement with the slope of a line through the high-temperature data. Since the calculated high-temperature behavior is largely determined by that part of the distribution of τ found in the vicinity of ω_0^{-1} , these results suggest that the cross-links introduce a substantial density of low-frequency components into the network motional frequency spectrum even at temperatures far above T_g .

The general expression for the network relaxation time over a broad range of temperature and cross-link density includes the chain contribution of each temperature and can be expressed in the form of eq 3 as

$$\begin{aligned} T_1^{-1} &= v_x A_x \int_0^\infty W_x(z) \tau^{*2} e^{2z} K(z) dz + (1 - v_x) A_c \\ &\quad \times \int_0^\infty W_c(z) \tau^{*2} e^{2z} K(z) dz \quad (9) \end{aligned}$$

where $K(z)$ represents the quantity in brackets in eq 7a. Each $W_j(z)$ contains the appropriate width parameter. When the distribution is Gaussian, eq 9 becomes

$$\begin{aligned} T_1^{-1} &= v_x (2A_x B_x \tau^* \pi^{-1/2}) \int_0^\infty \exp(z - B_x^2 z^2) K(z) dz + \\ &\quad (1 - v_x) (2A_c B_c \tau^* \pi^{-1/2}) \int_0^\infty \exp(z - B_c^2 z^2) K(z) dz \quad (10) \end{aligned}$$

where v_x , A_x , B_x , and A_c have their previous meaning. In using eq 10 we set $B_c = 20$; the distribution (eq 5) for CB-220 thus approximates a delta function. An assessment of the suitability of the distribution function and the spread parameter B_x is made by comparing the curves generated by eq 10 with the data. Two such curves, for which $B_x = 0.27$, are shown in Figure 4. The fit over the high- and low-temperature regions is good. The slopes are well reproduced, and it is clear that the difference in slope in the two temperature regions is a direct result of the asymmetry in the distribution of correlation times. The minima are not well reproduced in magnitude. This is to be expected since the analytic function used to approximate T_1 vs. $1/T$ for the free chains does not accurately describe the data in that region.

Only at values of $v_x \gtrsim 0.4$, when $N \lesssim 7.5$, is it necessary to alter the width of the distribution by decreasing B_x in order to describe the data. In this region the mobility of the cross-link itself is diminished because of its proximity to other cross-links. An extreme case is sample 6 for which our measurements indicate a temperature-independent limiting value of $T_1 \approx 55 \text{ ms}$. In this region of cross-link concentration all of our expressions and approximations break down; the values of N have approximate meaning only, and the central assumption of a cross-link being a well-defined entity whose properties are independent of network chains is inapplicable.

Three conclusions follow from the above analysis of the data in the region $N \gtrsim 7.5$: (a) the cross-links may be viewed as independent entities; (b) the distribution of τ 's associated with the cross-link region is very broad (B_x equal to 0.27 corresponds to a distribution whose rms width extends up to about

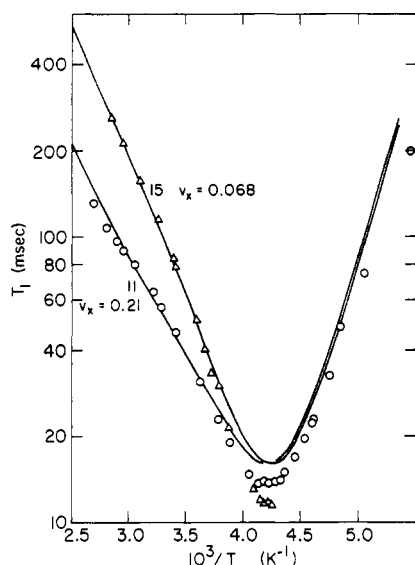


Figure 4. Proton relaxation data for cross-linked PB samples 15 (Δ) and 11 (\circ) compared with the computed results from eq 10. The samples have average network chain lengths of 44 and 14 repeat units, respectively. For more lightly cross-linked samples ($N > 44$, not shown) the fit is excellent.

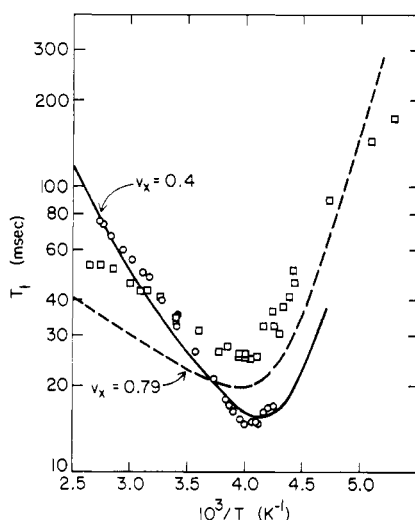


Figure 5. Proton relaxation data for very heavily cross-linked samples 19 (\circ) and 8 (\square) containing chains approximately 7.5 and 3.8 repeat units long, respectively. The curves are from eq 9 using parameters given in the text.

$14\tau^*$); and (c) the relaxation behavior of the chain segments in a network is well described by the relaxation of uncross-linked CB-220.

At temperatures below that of the T_1 minimum the chain segments represent the sites of shortest relaxation time and the effect of adding cross-links is primarily subtractive in the sense that it diminishes the concentration of free chains and thus increases T_1 by shifting the average $\bar{\tau}$ of the distribution away from ω_0^{-1} . The sharp cutoff at the short τ end of the proposed distribution is evident from the rapidly increasing T_1 at low temperature for all $N \geq 3.8$ (Figure 1). The curves for T_1 lie parallel to each other in this region, and T_1 increases with N at fixed T . Again there is no evidence for $\tau < \tau_c$ in the cross-linked network.

There are ambiguities about the nature of the cross-link region as it is characterized here, but if our model is correct it is just that region of the elastomer which supports those

motional correlation times greater than and down to the chain segmental correlation time. The density function $P(\tau)$ for cross-links excludes those components arising from the chain and simultaneously fixes the definition of the cross-link concentration.

For $v_x \geq 0.4$ the constraints on the chains which lie outside of the cross-link regions rapidly increase. As a consequence, proton relaxation in these chains cannot be satisfactorily approximated by the relaxation behavior of CB-220. The data for sample 19 are compared in Figure 5 with the results of eq 10 using $B_x = 0.27$ and $v_x = 0.4$. The disagreement here is most noticeable in the pronounced curvature of the calculated curve; at this concentration and above, the cross-links inhibit the motion of the connecting chain repeat units and in addition the cross-link regions interact and perturb each other. At these high cross-link concentrations it becomes necessary in our phenomenological approach to allow B_c and B_x to vary with N , or to replace the two distribution functions by a single more suitable choice. We use the former approach in trying to fit the data for sample 8, for which $3/N = 0.79$. Using eq 9 with $E_x = 1$, $B_x = 0.20$, $E_c = 2$, $B_c = 20$ the broken curve shown in Figure 5 is obtained. Although the absolute magnitude of T_1 is not in good agreement, the temperature dependence is reasonable.

IV. Summary and Discussion

We have measured the proton dipolar spin-lattice relaxation as a function of cross-link density and temperature in *cis*-1,4-polybutadiene. The single, deep minimum in the spin-lattice relaxation in the uncross-linked material is the result of segmental motion. At temperatures higher than the temperature at the T_1 minimum marked reduction in T_1 with cross-linking was observed. However, under no circumstances was T_1 smaller than the $T_{1\min}$ of uncross-linked PB. The fact that the slope of the $\log T_1$ vs. $1/T$ plot decreased with increased cross-link density may relate to the inequality of the high- and low-temperature slopes in *uncross-linked* PB where entanglements cause some motional constraint.

The model on which our interpretation is based relies on spin diffusion to locations of rapid spin-lattice relaxation. At high temperatures these locations are the cross-links; at low temperatures the network chain segments provide the most effective relaxation. Motional frequency components near ω_0 are always present in the high-temperature region but are apparently greatly diminished or absent when the chain segmental frequencies drop below approximately ω_0 . We conclude that cross-links introduce a broad distribution of correlation times extending toward longer times and that few if any components shorter than the chain segmental times are present in cross-linked PB. The model used here assumes a monodisperse network in which we treat the average network chain length as if it were applicable to each chain. We have briefly discussed cross-link RU fractions greater than $v_x = 0.3$ largely to demonstrate that even at high cross-link densities, where our definitions of "isolated cross-link region" and "free chain region" break down, the relaxation process can be reasonably well approximated by the model proposed.

Lind¹⁸ in a recent paper reports a room-temperature NMR study of an alternating block copolymer of 35 wt % bisphenol-A polycarbonate (BPAC) and 65 wt % poly(dimethylsiloxane) (DMS). The relaxation mechanism he describes is very similar to that employed here with the rigid BPAC taking the role of our cross-link region as the rapid relaxation site. A more sophisticated model would treat the magnetization gradients explicitly especially at temperatures or cross-link densities where moderate magnetization gradients exist over a large proportion of the network chains.

Acknowledgment. We wish to express our gratitude to R. J. Gaylord for many helpful conversations and suggestions and

to D. Lohse for his continued interest; also we wish to thank B. Crist for useful comments. The B. F. Goodrich Co. generously supplied the *cis*-polybutadiene starting material, CB-220. This work was supported in part by the U.S. Energy Research and Development Administration, Contract EY-76-C-02-1198.

References and Notes

- (1) H. S. Gutowsky, A. Saika, M. Takeda, and D. E. Woessner, *J. Chem. Phys.*, **27**, 534 (1957).
- (2) H. S. Gutowsky and L. H. Meyer, *J. Chem. Phys.*, **21**, 2122 (1953).
- (3) N. Bloembergen, E. M. Purcell, and R. V. Pound, *Phys. Rev.*, **73**, 679 (1948).
- (4) C. S. M. Ong and R. S. Stein, *J. Polym. Sci., Part A-2*, **12**, 1599 (1974).
- (5) P. J. Flory and J. Rehner, Jr., *J. Chem. Phys.*, **11**, 521 (1943); P. J. Flory, "Principles of Polymer Chemistry", Cornell University Press, Ithaca, N.Y., 1953.
- (6) L. D. Loan, *Rubber Chem. Technol.*, **40**, 149 (1967).
- (7) A more lengthy and detailed discussion of eq 1 together with considerations leading to our choice of $A = 1$ and $B = 0.5$ can be found in the Ph.D Thesis of L. C. Labun (submitted to the University of Illinois in 1976). The latter includes a table in which the ν_e resulting from various choices of A and B are compared.
- (8) D. W. McCall, *Acc. Chem. Res.*, **4**, 223 (1971).
- (9) J. P. Cohen-Addad and J. P. Faure, *J. Chem. Phys.*, **61**, 1571 (1974); Y. Martin-Borret, J. P. Cohen-Addad, and J. P. Messa, *ibid.*, **58**, 1700 (1973).
- (10) S. Kaufman, W. P. Slichter, and D. D. Davis, *J. Polym. Sci., Part A-2*, **9**, 829 (1971).
- (11) B. Crist and A. Peterlin, *J. Macromol. Sci., Phys.*, **4**, 791 (1970).
- (12) H. A. Resing, *J. Chem. Phys.*, **43**, 669 (1965).
- (13) A. Abragam, "The Principles of Nuclear Magnetism", Clarendon Press, Oxford, 1961, p. 289 ff.
- (14) R. Lenk and J. P. Cohen-Addad, *Solid State Commun.*, **8**, 1869 (1970).
- (15) J. Jonas and Nan-I Liu, *J. Magn. Reson.*, **18**, 444 (1975).
- (16) T. M. Connor, *Trans. Faraday Soc.*, **60**, 1574 (1964).
- (17) W. Weibull, *J. Appl. Mech.*, **18**, 293 (1951).
- (18) A. C. Lind, *J. Chem. Phys.*, **66**, 3482 (1977).

Topological Structure and Physical Properties of Permanently Cross-Linked Systems.

1. s-Functional, Homogeneous, Gaussian Systems

Andrzej Ziabicki*^{1a} and Janusz Walasek^{1b}

Polish Academy of Sciences, Institute of Fundamental Technological Research, 00-049 Warsaw, Poland, and Technical University, Department of Physics, 26-600 Radom, Poland. Received November 21, 1977

ABSTRACT: Topological structure of homogeneous, permanently cross-linked systems has been described in terms of the distribution of various structural elements (single, double, etc., chains connecting pairs of junctions, free-end chains, loops, and void functionalities). For a system with *s*-functional junctions general formulas have been derived for the critical structure (gel point), chain-contraction coefficient, concentration of elastically effective junctions, modulus of elasticity, and gel fraction.

It was recognized many years ago that the topological structure of rubber networks affects their elasticity, gel-sol fraction, and other macroscopic properties. Flory,^{2a} Tobolsky,^{2b} Case,³ Scanlan,⁴ Mullins and Thomas,⁵ Dobson and Gordon,⁶ and others^{7,8} introduced various corrections to the equations of rubber elasticity, to allow for the presence of elastically ineffective parts of cross-linked systems, due to free-end chains connected to cross-links with one end only. The present author discussed tetrafunctional networks with free-end chains and loops⁹ and together with Klonowski¹⁰ tried to derive information about the distribution of cross-links with various numbers of such structural elements from thermodynamic considerations (minimization of free energy)¹⁰ to obtain "thermodynamically most probable structures". It was realized later that such an approach was not applicable to permanent, irreversible networks, as for such systems, no mechanism for thermodynamic optimization is available. Also, free-end chains and loops, discussed in the earlier papers, do not exhaust all topologically admissible types of structural elements, and analyses emphasizing only some types of junctions and neglecting others are rather arbitrary. Therefore, we have considered the problem once more to give a more systematic analysis of cross-linked systems with all topologically possible structural elements. The present analysis is an extension and generalization of the earlier treatment by the author and Klonowski^{9,10} which now includes correction of errors resulting from the thermodynamic approach, inadmissible to permanently cross-linked systems. The present paper concerns cross-linked systems of any functionality,

presents general classification of topologically possible defects, and derives general expressions for modulus of elasticity G , contraction coefficient A , critical structure (gel point), and gel fraction. Further papers in this series will deal with more specific network models for which the distribution functions will be derived from additional assumptions.

Characterization of Cross-Linked Structures

Consider a set of chains \mathcal{C} (with cardinality N_c) and a set of cross-links (junctions) \mathcal{J} (with cardinality N_j). Chains connected with their ends to cross-links form the system under consideration. There are several different ways in which the chains can be connected to various junctions. Considering a single cross-link one can distinguish several "structural elements" attached to it (Figure 1). *Uncross-linked* chains, strictly speaking, do not form part of the cross-linked system, but, being present in all real systems, contribute to their physical behavior. The elements which occupy a single functionality at each junction are: singlets, i.e., chains connected with their two ends to two different cross-links (s), free-end chains (f), i.e., chains connected with one end to one junction only, and void functionalities (v). The elements consuming two functionalities of each cross-link to which they are connected are: doublets (d), i.e., two chains connecting the same pair of junctions, and loops, (l), i.e., chains connected with both ends to the same cross-link. Triplets (t), quadruplets (q), and higher multiplet parallel groups of three, four, or more chains connecting the same pair of cross-links appear in systems of cross-links with higher functionalities.